Available online at www.sciencedirect.com

ScienceDirect

Procedia Structural Integrity 26 (2020) 269–276

Structural Integrity Procedia

www.elsevier.com/locate/procedia

The 1st Mediterranean Conference on Fracture and Structural Integrity, MedFract1

Bending behavior of AM50 Magnesium alloy under static and dynamic loading

Sergiu-Valentin Galatanu[a], Milena Scano[b], Daniel Pietras[c], Liviu-Daniel Pirvulescu[a], Maria Cristina Porcu[b], Liviu Marsavina[a,]*, Tomasz Sadowski[c]

[a] *University Politehnica Timisoara, 1 Mihai Viteazul Blvd., 300222, Timisoara, Romania*
[b] *University of Cagliari, 40 Via Università, 09124 Cagliari, Italy*
[c] *Lublin University of Technology, Nadbystrzycka 38 D, 20 – 618 Lublin, Poland*

Abstract

Thanks to their excellent stiffness, high ductility and strength-to-weight ratios, Magnesium alloys are increasing their applications in different fields, from automotive to aerospace and biomedical engineering. Particularly, in automotive industry the Magnesium alloys are used for steering wheel skeletons, which are mainly loaded in bending and torsion. Therefore, investigating on the bending and torsional properties of Magnesium alloys under static and dynamic loading is crucial for practical applications. This paper presents the results of an experimental program on AM50 Magnesium alloy specimens, tested under quasi-static and dynamic loading. Three-point quasi-static and dynamic bending tests were conducted on rectangular specimens. A loading speed of 1 mm/s was assumed in the quasi-static tests. The dynamic tests were carried out by drop weight with three different loading speeds (1, 3 and 5 m/s). The post-elastic behavior of the material was investigated, estimating the load carrying capacity, ductility and energy absorption and by comparing the results obtained under dynamic and static conditions.

Keywords: Non-ferrous metals and alloys; bending tests; dynamic tests

* Corresponding author. Tel.: +40-256-403577; fax: +40-256-403523.
E-mail address: liviu.marsavina@upt.ro

10.1016/j.prostr.2020.06.034

1. Introduction

Thanks to their excellent stiffness, high ductility and strength-to-weight ratios, Magnesium alloys are increasing their applications in different fields, from automotive to aerospace and biomedical engineering, Kulekci (2008), Monteiro (2011), Dvorsky et al. (2019). On the other hand, Magnesium alloys have been adopted both for structural and nonstructural components since from the end of the 19th century, ranging from nautical and aeronautical industry to automotive and civil engineering applications, Mazzolani (2004). Merging the potential properties of the two principal constituent materials together, Magnesium-Aluminum alloys have proven to be competitive with other structural materials, Easton ET AL (2006), characterized as they are by high resistance to corrosion, good mechanical properties and remarkable energy-absorbing capacity.

Among commercial Magnesium-Aluminum cast alloys, AM50 is one of the most used in practical applications. Several experimental and numerical studies have been developed in the last years on AM50 Magnesium alloys, to investigate the material microstructure, Kiełbus et al. (2006), Wang et al. (2003), tensile ductility Lee et al. (2005), dissipative properties Kaczyński et al. (2019), fatigue behavior Chen et al. (2007), Marsavina et al. (2019), mechanical behavior Serban et al (2019), as well as corrosion phenomena Liang et al. (2009). Experimental tests to investigate the fatigue crack growth micro mechanisms in high-pressure die-cast AM50 alloy were also carried out by El Kadiri et al. (2006).

Although some key aspects of the behavior of such materials have been widely investigated, further studies are needed to better understand their behavior under extreme conditions of loads, when high inelastic deformations are achieved, and local damage phenomena take place. The purpose of this paper is to determine the properties of AM50 Magnesium alloy under static and dynamic bending tests. In particular, the post-elastic behavior of the material is studied, while strength, ductility and energy absorption are estimated, the latter being crucial properties of materials and structures, Ghiani et al (2018), Porcu (2017), Porcu et al. (2012, 2019). The influence of the test speed for dynamic loading is also investigated. The static tests were carried out according with ASTM E290-97 standard.

The paper is divided into three sections. The first two present procedures and results of the static and dynamic bending tests on AM50 Magnesium alloy, while the main conclusions are summarized in the last section.

2. Experimental methods

For the mechanical characterization of the AM50 Magnesium alloy, 15 casting networks according to Fig. 1.a were used. Each casting network is composed of 6 specimens:

- Two Type 1 specimens with rectangular section used for tensile and bending tests, see Fig. 1.b.
- Two Type 2 specimens with circular section (12 mm diameter on the calibrate area), used for tensile and rotating-bending fatigue.
- Two Type 3 specimens with circular section (6.5 mm diameter on the calibrate area), used for torsion and axial fatigue. Due to some problems with the separation plan, however, only one of them was suitable for the tests.

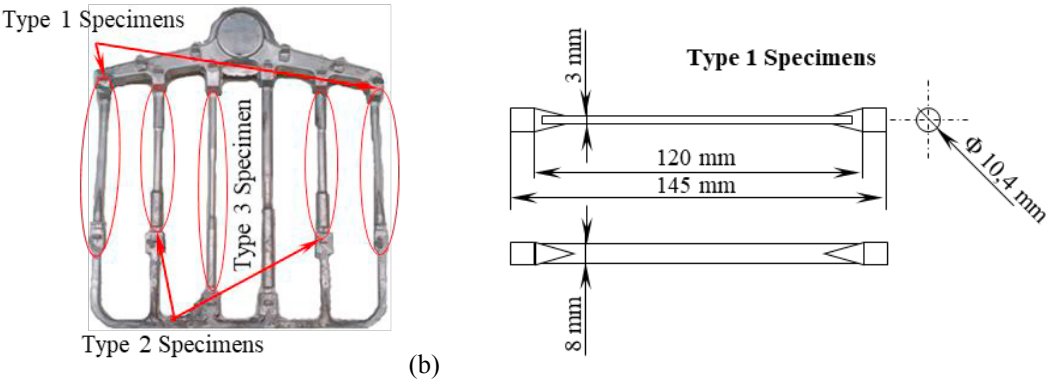

Fig. 1. (a) Casting network; (b) Type 1 specimen with rectangular section.

The specimens were casted under pressure in the same conditions and technological parameters used to obtain the steering wheels.

Type 1 specimens with rectangular section (see Fig. 1b) were used for three-point bending tests under static and dynamic loading.

2.1. Static Tests

The static three-point bending tests were performed by means of the Universal Test Machine Zwick/Roell Z005 having 5 kN maximum force, equipped with two supports and one mandrel, as shown in Fig. 2. A schematic representation of the three-point test is given in Fig. 2.a, where both the initial and the final configurations are illustrated. Two pictures taken at the start and at the end of the test are provided in Fig. 2.b and 2.c, while the deformed specimens are displayed in Fig. 2.d.

With reference to the parameters in Fig. 2, the distance between supports is given by the formula:

$$\ell = (D + 3h) + \frac{h}{2} = 30.5\ mm \tag{1}$$

where D is the diameter of the mandrel or plunger (20 mm) and a is the sheet specimen thickness (3 mm). Tests were performed at room temperature (23°C) with a loading speed of 1 mm/s according to ASTM E290–97. The bending force was applied slowly to allow plastic deformation of the material. Bending test was stopped when an angle α of 120º was reached, Fig. 2 (d).

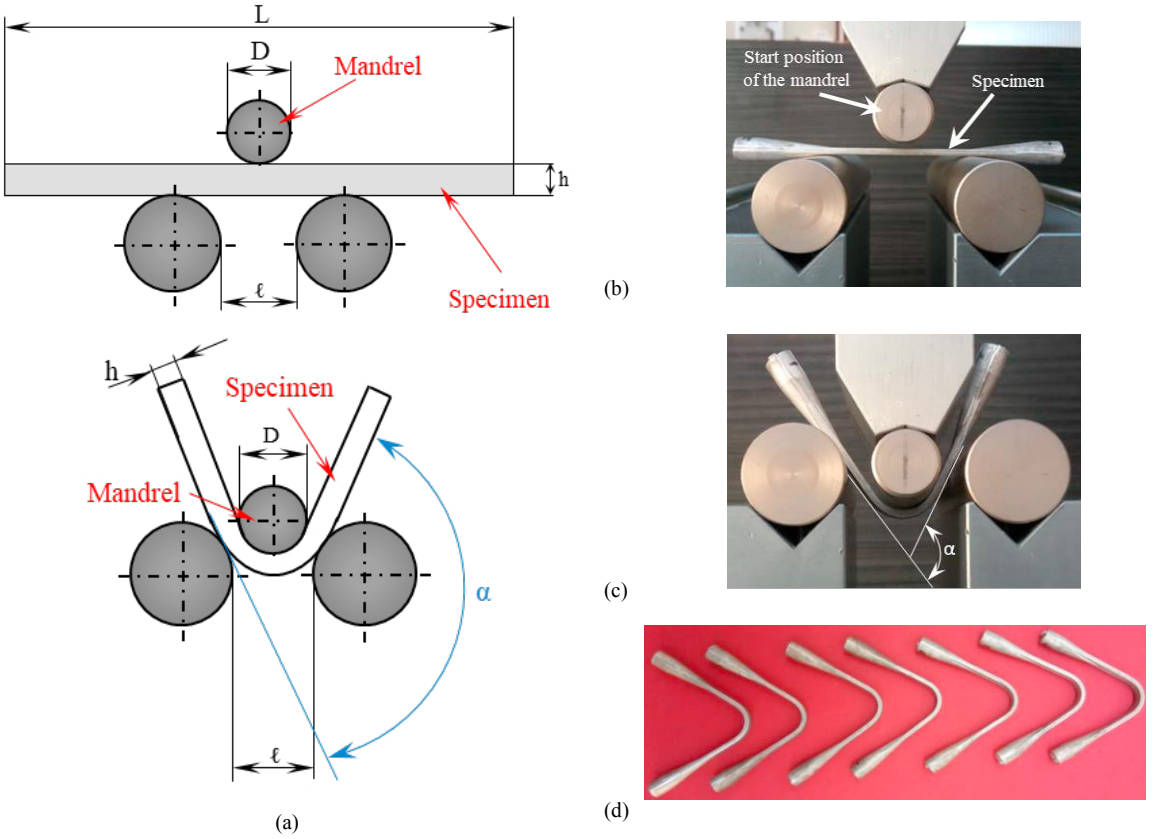

Fig. 2. (a) Schematic representation of three-point bending test, (b) initial configuration; (c) final configuration; (d) Specimens after the static bending tests.

2.2. Dynamic Tests

Dynamic response of the AM50 Magnesium Alloy was assessed in three-point bending conditions by using Instron Dynatup 9210 drop tower. The test stand with damaged specimen is shown in Fig 3. For each test the span between specimen supports was equal to 62 mm. The impact velocity is adjusted up to 5 m/s by the initial height of dropped weight and impactor. The investigations were performed for loading speeds of 1 m/s, 3 m/s and 5 m/s.

The test starts when the dropped weight (having mass m) is released from the handle. When the impactor reaches a position very close to the specimen surface, its velocity is recorded and carrying force $p(t)$ acquisition starts. The total force F is defined as the algebraic sum of gravity force and $p(t)$, that is:

$$F = mg - p(t) \tag{2}$$

The actual impact velocity $v(t)$ is computed according to the universal gravitation law, by considering the gravitational acceleration g and the time interval between the time when the velocity was recorded and the time when the carrying force was measured by the transducer. From the latter time onwards, the loading velocity $v(t)$ starts to decrease and the specimen deforms.

The displacement $\delta(t)$ during impact can be defined as the area under the velocity $v(t)$ curve, which makes necessary to measure the force $p(t)$ and the dropped mass m. The displacement can be computed by integration of velocity:

$$\delta(t) = \int v(t)dt = \frac{1}{2}gt^2 - \frac{1}{m}\iint p(t)dtdt \tag{3}$$

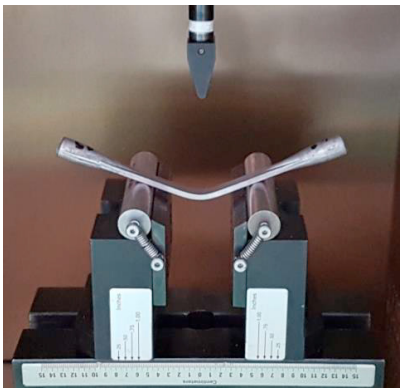

Fig. 3. Dynamic three-point bending test stand with damaged specimen

3. Results and discussions

3.1. Static Tests Results

The force–displacement curves obtained from the static bending tests carried out on seven Type 1 specimens are given in Fig. 4. Curves in Fig. 4 highlights a good correlation between the results obtained for the different specimens. Table 1 compares the values of maximum force and displacement at the maximum force obtained for each specimen. In the same table, the values of the ductility, defined as the ratio between the displacement at maximum force and the displacement at yield, and of the energy absorption, calculated as the area below the curve excluding the elastic energy, are also provided.

The average values are provided in the last row of Table 1, while the higher and the lower values are evidenced in bold black and bold blue, respectively.

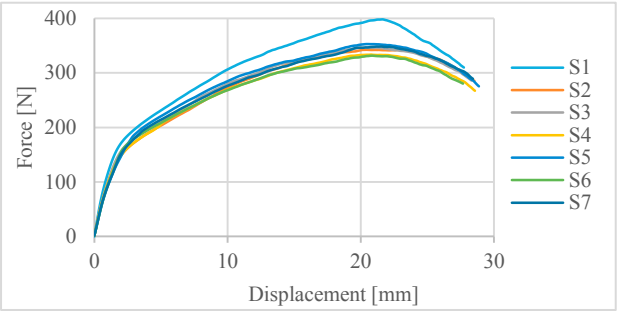

Fig. 4. Force–Displacement curves obtained for seven specimens under static bending tests

Table 1. Bending properties obtained from static tests.

Specimen	Test Speed [m/s]	Maximum Force F_{max} [N]	Displacement at the maximum force δ [mm]	Absorbed energy at the maximum force W [J]	Ductility [-]
S1	0.001	**398.23**	**21.62**	**6.27**	**19.15**
S2	0.001	342.42	**20.45**	**5.14**	18.76
S3	0.001	346.25	22.94	5.21	**15.31**
S4	0.001	333.54	20.77	5.15	17.33
S5	0.001	352.84	20.49	5.34	16.37
S6	0.001	**331.71**	20.90	5.19	16.15
S7	0.001	348.43	21.56	5.59	17.52
Average		**350.49**	**21.25**	**5.41**	**17.23**

3.2. Dynamic Tests Results

The force-displacement curves obtained for three different specimens (namely, SD10, SD3, SD12) under dynamic bending tests are given in Fig. 5. The curves are plotted for different values of test speed in m/s: 1, 3, 5. For comparison, the force-displacement curve obtained for the quasi-static test referred to as S1 in Fig. 4, is also plotted in the same figure.

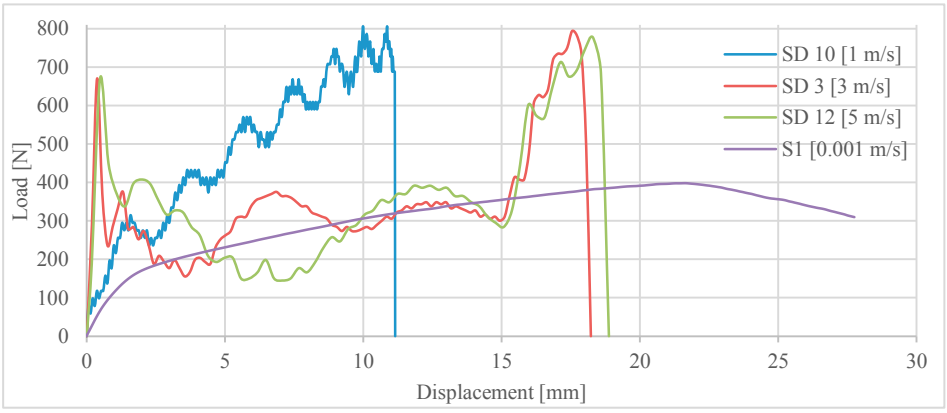

Fig. 5. Force – Displacement curves obtained for specimens under dynamic bending tests. The quasi-static curve is also provided for comparison in the figure.

In Table 2 are listed the values of maximum force, displacement and absorbed energy (under the maximum force) obtained for each specimen. The higher and lower values are again evidenced in bold black and bold blue, respectively.

Table 2. Bending properties obtained for dynamic tests.

Specimen	Test Speed [m/s]	Maximum Force F_{max} [N]	Displacement at the maximum force δ [mm]	Absorbed energy at the maximum force W [J]	Ductility [-]
SD 10	1	**806.46**	**10.86**	**4.26**	**8.37**
SD 3	3	793.86	17.54	5.45	13.19
SD 12	5	**777.77**	**18.3**	**5.82**	**13.76**
S1 (quasi-static test)	0.001	**398.23**	**21.62**	**6.27**	**19.15**

3.3. Discussion of results

The static three-point bending tests were performed according to ASTM E290 – 97 in order to evaluate maximum load, ductility, absorbed energy and the presence of damage on the surfaces. No imperfections or cracks were detected on the specimens' surfaces after the tests, at least to a visual (non-microscopic) analysis. A rather high extent of ductility and energy absorption was observed during the static tests. Curves in Fig. 4 show that almost the same value of maximum load, ductility and energy absorption are exhibited by different specimens under static loads, as also shown by Table 1, except for S1 specimen that showed slightly higher values. On average, during quasi-static tests, the maximum load was about 350 N, ductility 17.23 and energy absorption 5.41 J.

As far as the dynamic bending tests are concerned, it can be noted that the load-displacement curves obtained with test speed of 3 m/s and 5 m/s (red and green curves in Fig. 5) were very similar, while the constitutive curve relevant to 1 m/s speed (blue curve in Fig.5) exhibited a different pattern. The first peak appearing at very low values of displacement in both the red and green curves is due to some initial settlements of the specimens, so this part of the curves was not considered when calculating the yield displacement. The last peak appearing in the same curves corresponds to the maximum value of the load instead, which caused the specimen fracture. On the contrary, no initial peak appears in the blue curve where the maximum load value is reached more uniformly through shock waves.

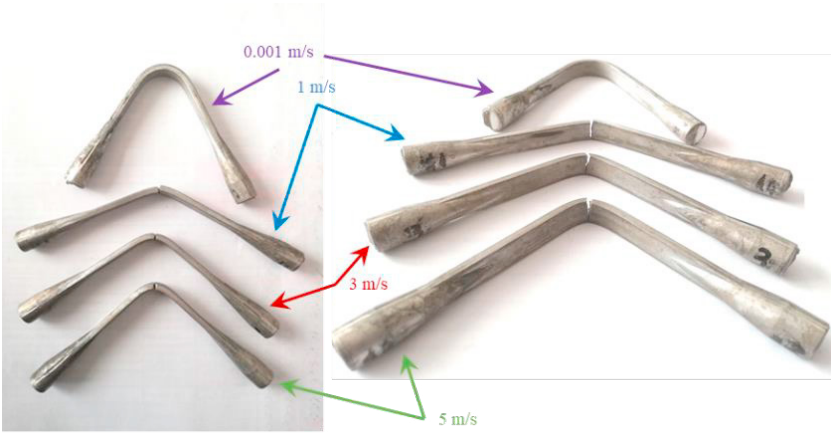

Fig. 6. Specimens after the testing

Curves in Fig. 5 show that the extent of the plastic deformation increases as the test speed increases. The ductility ranges, in fact, from 8.37 for 1 m/s test speed to 13.76 for 5 m/s test speed, while the absorbed energy increases from 4.26 J to 5.82 J. On the contrary, the maximum load reached during the test, is almost the same for the three considered dynamic tests (about 800 N). When the test is conducted under quasi-static conditions (0.001 m/s speed),

the maximum load is almost half (about 400 N), while the ductility almost doubles reaching the value of 19.15, with an amount of absorbed energy of 6.27 J. It is worth noting that, the absorbed energy during static and dynamic tests was almost the same, despite of the different extent of the plastic deformation.

The average value of the absorbed energy (7 quasi-static tests and 3 dynamic tests for each speed: 1, 3 and 5 m/s) is presented in Fig. 7, which shows a good ability to absorb energy for AM50 Magnesium alloy. This represents an important advantage of AM50 Magnesium alloy used in safety systems from automotive industry.

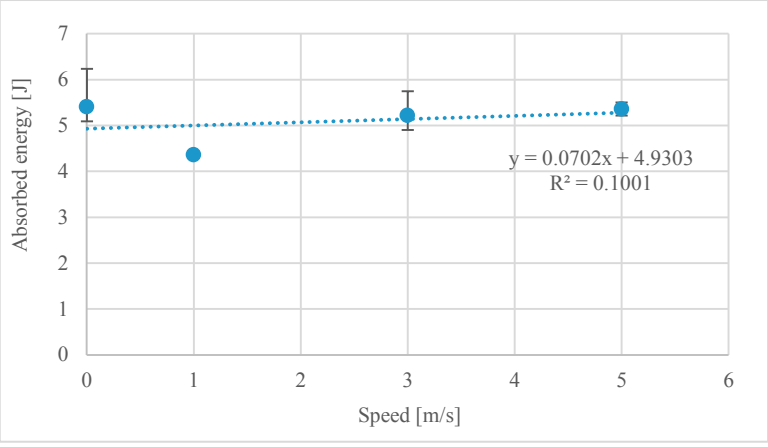

Fig. 7. Average values of absorbed energy for different test speeds

4. Conclusions

The paper presents the results of an experimental investigation carried out on AM50 Magnesium alloy specimens. Both quasi-static and dynamic tests were conducted on different specimens die casted with the same technological parameters and kept in the same environmental conditions, as steering wheel skeletons. The results show in general a good ductility and capacity to absorb energy for AM50 Magnesium alloy.

The following conclusions could be drawn:

1. The maximum force achieved during dynamic bending tests is on average about 800 N. When the test is conducted under quasi-static condition, it is almost half (about 400 N).
2. Under dynamic tests, the ductility and the absorbed energy increase as the test speed increases, reaching their maximum values (13.76 and 5.82 J, respectively) for 5 m/s test speed.
3. Under quasi-static tests, however, the ductility exhibited by the material is higher (up to 19.15) than under dynamic tests.
4. On contrary, the absorbed energy during static and dynamic tests was, on average, almost the same (about 5 J), despite of the different extent of the plastic deformation.
5. Under dynamic tests, all the specimens were broken at almost the same maximum load, regardless the test speed. However, the specimens reached a different value of bending angle α under different test speed, due to the different post-elastic behavior (maximum displacement and extent of the plastic range) exhibited by the specimens when tested with different speed, Fig. 6.

The results of the present paper add new elements to the knowledge of the behavior of AM50 Magnesium alloy under bending tests. Evidences found in the literature show that under tensile tests the yield strength of most metals and alloys typically increases as strain rate increases, while a decrease in ductility (and even a transition from ductile to brittle fracture) is often associated to the increase of strain rate, Davis (2004). The results of the present study confirm the increase of yield strength with test speed for AM50 Magnesium alloy under bending tests. Although the ductile behavior of such alloy seems to improve with test speed, however, higher values of ductility are found when static tests are performed, due to a higher inelastic deformation of specimens.

Of course, further experimental investigations are needed to make the present conclusions more robust and general.

Acknowledgements

The authors are gratefully for the financial support of Bridge Grant of the Romanian National Authority for Scientific Research, CNCS-UEFISCDI, contract number 89 BG/2016, for the support of TRW Automotive Safety Systems SRL Timişoara and to the European Union's Horizon 2020 research and innovation programme under grant agreement No 857124. The Erasmus Traineeship Program of the University of Cagliari is also acknowledged.

References

ASTM E290-97a (2004), Standard Test Methods for Bend Testing of Material for Ductility, ASTM International, West Conshohocken, PA, 2004, www.astm.org

Chen, L., Wang, C., Wu, W., Liu, Z., Stoica, G. M., Wu, L., & Liaw, P. K. (2007). Low-cycle fatigue behavior of an as-extruded AM50 magnesium alloy. Metallurgical and Materials Transactions A, 38(13), 2235-2241.

Davis, J. R. (Ed.). (2004). Tensile testing. ASM international.

Dvorsky, D., Kubasek, J., Jablonska, E., Lipov, J., & Vojtech, D. (2019). High strength AM50 magnesium alloy as a material for possible stent application in medicine. Materials Technology, 34(14), 838-842.

Easton, M., Song, W. Q., & Abbott, T. (2006). A comparison of the deformation of magnesium alloys with aluminium and steel in tension, bending and buckling. Materials & design, 27(10), 935-946.

El Kadiri, H., Xue, Y., Horstemeyer, M. F., Jordon, J. B., & Wang, P. T. (2006). Identification and modeling of fatigue crack growth mechanisms in a die-cast AM50 magnesium alloy. Acta Materialia, 54(19), 5061-5076.

Ghasemi, A., Raja, V. S., Blawert, C., Dietzel, W., & Kainer, K. U. (2008). Study of the structure and corrosion behavior of PEO coatings on AM50 magnesium alloy by electrochemical impedance spectroscopy. Surface and Coatings Technology, 202(15), 3513-3518.

Ghiani, C., Linul, E., Porcu, M. C., Marsavina, L., Movahedi, N., & Aymerich, F. (2018). Metal Foam-Filled Tubes as Plastic Dissipaters in Earthquake-Resistant Steel Buildings. In IOP Conference Series: Materials Science and Engineering (Vol.416, No.1, p.012051). IOP Publishing.

Kaczyński, P., Gronostajski, Z., & Polak, S. (2019). Progressive crushing as a new mechanism of energy absorption. The crushing study of magnesium alloy crash-boxes. International Journal of Impact Engineering, 124, 1-8.

Kiełbus, A., Rzychoń, T., & Cibis, R. (2006). Microstructure of AM50 die casting magnesium alloy. Journal of Achievements in Materials and Manufacturing Engineering, 18(1-2), 135.

Kulekci, M. K. (2008). Magnesium and its alloys applications in automotive industry. The International Journal of Advanced Manufacturing Technology, 39(9-10), 851-865.

Lee, S. G., Patel, G. R., Gokhale, A. M., Sreeranganathan, A., & Horstemeyer, M. F. (2005). Variability in the tensile ductility of high-pressure die-cast AM50 Mg-alloy. Scripta materialia, 53(7), 851-856.

Liang, J., Srinivasan, P. B., Blawert, C., Störmer, M., & Dietzel, W. (2009). Electrochemical corrosion behaviour of plasma electrolytic oxidation coatings on AM50 magnesium alloy formed in silicate and phosphate-based electrolytes. Electrochimica Acta, 54(14), 3842-3850.

Marsavina, L., Iacoviello, F., Pirvulescu, L. D., Di Cocco, V., & Rusu, L. (2019). Engineering prediction of fatigue strength for AM50 magnesium alloys. International Journal of Fatigue, 127, 10-15.

Mazzolani, F. M. (2004). Competing issues for aluminium alloys in structural engineering. Progress in Structural Engineering and Materials, 6(4), 185-196.

Monteiro, W. A. (Ed.). (2011). Special issues on magnesium alloys. InTech, 2011.

Porcu, M. C. (2017). Ductile behavior of timber structures under strong dynamic loads. Wood in Civil Engineering. Rijeka: InTechOpen, 173-196.

Porcu, M. C., & Carta, G. (2012). A better rigid-plastic estimate for earthquake-induced plastic displacements. International Journal of Safety and Security Engineering, 2(2), 184-196.

Porcu, M. C., Vielma, J. C., Panu, F., Aguilar, C., & Curreli, G. (2019). Seismic retrofit of existing buildings led by non-linear dynamic analyses. International Journal of Safety and Security Engineering, 9(3), 201-212.

Şerban, D. A., Marsavina, L., Rusu, L., & Negru, R. (2019). Numerical study of the behavior of magnesium alloy AM50 in tensile and torsional loadings. Archive of Applied Mechanics, 89(5), 911-917.

Wang, R. M., Eliezer, A., & Gutman, E. M. (2003). An investigation on the microstructure of an AM50 magnesium alloy. Materials Science and Engineering: A, 355(1-2), 201-207.